

PRELIMINARY ASSESSMENT OF THE GEOMETRIC PERFORMANCE OF SATELLITE DATA IMAGED BY AVNIR-ADEOS

Subaryono¹, Suta'at, Djurdjani¹, Priyono Nugroho¹

ABSTRACT

In August 1996 the National Space Development Agency of Japan (NASDA) launched its satellite called the Advanced Earth Observation Satellite (ADEOS) carrying a very high spatial resolution sensor named AVNIR (Advanced Visible and Near-Infrared Radiometer). This sensor is capable of recording the earth surface with pointing angle ± 40 degrees perpendicular to the satellite flight direction. These characteristics are particularly attractive to develop a three-dimensional model from a pair of overlapped AVNIR images taken from two adjacent paths. However, in order to be used to generate a representative Digital Elevation Model (DEM) the geometric performance of the data imaged by this sensor need to be evaluated. This research assesses such performance.

A pair of overlapped panchromatic AVNIR satellite images were used as samples. Coordinate transformation algorithms including Affine, Projective, and Polynomial were developed to rectify the images. Ground control points (GCPs) acquired from topographic maps were used as input into those three algorithms. In this case, the Root Mean Square Error (RMSE) of each algorithms applied in the left and right images indicate the image geometric performance. Furthermore, this research attempts to determine the B/H ratio of the images. A mathematical model representing collinearity conditions among objects on the ground and their corresponding points on the image was used.

1. INTRODUCTION

The National Space Development Agency of Japan (NASDA) successfully launched its earth observation satellite called the Advanced Earth Observation Satellite (ADEOS) in August 1996. The ADEOS has been designed for observing, monitoring and analysing global warming, ozone depletion and extreme weather, in view of the future forecasting of these global phenomena. The 4m x 4m x 5m dimensions of this satellite have appeared as the largest satellite Japan has ever developed. The ADEOS carries 8 sensors with different purposes, i.e., OCTS, AVNIR, IMG, ILAS, RIS, NSCAT, TOMS and POLDER.

This research has focused on the data imaged by AVNIR (Advanced Visible and Near-Infrared Radiometer). This sensor is a pushbroom type that scans the earth surface

using a linear array of pixels on the focal plane. The most important characteristics of AVNIR are its high spatial resolution and sensor pointing function. The AVNIR instantaneous field of views (IFOV) for the Mu band and Pa band are 20 μ rad (approximately 16 m surface distance) and 10 μ rad (approximately 8 m surface distance). The pointing function can be operated within an area of ± 40 degrees perpendicular to the satellite flight direction (Nakamura, 1997).

The AVNIR characteristics, particularly its pointing angle function, are quite attractive because they can produce pairs of overlapped images with good proportions of B/H (base-height) ratio. This condition is necessary to generate three dimensional models known as digital elevation models (DEM) and to extract the elevation data for topographic mapping. However, in order to be used to generate DEM that represent the real world the geometric performance of the data imaged by this sensor needs to be evaluated.

Generally, four main steps are necessary to generate a DEM from a pair of overlapped images, they are: (1) data preparation, (2) orientation of a stereo pair, (3) computation of parallax, and (4) generation of DTM. In conducting steps 2 to 4, several methods can be applied, and are still open to be developed and refined (Rao et al, 1996; Toshiaki, 1997, Prof. Murai: personal communication, 1997). This research conducted a preliminary stage of assessing the geometric performance of the data imaged by AVNIR to generate a DEM focusing on the step 2, e.g., the orientation of stereo pair. This step is very crucial since the ADEOS is polar orbiting satellite which its adjacent paths are not parallel. The assessment apply the digital photogrammetric approach including coordinate transformation and space resection methods.

2. METHODOLOGY

Two main parts of this assessment are (1) digital rectification or in this case, is the establishment of epipolar geometry, and (2) computation of B/H ratio. They are described below:

2.1. Digital Rectification

One of the pre-requisite to generate a three-dimensional model is the establishment of epipolar geometry. This includes efforts to remove y-parallax on the images. Two types of parallax commonly occurs in a pair of overlapped images are: y-parallax, due to the platform motion, and x-parallax due to terrain relief. To generate a DEM, it is necessary to remove y-parallax so that only x-parallax exists in horizontal direction. This process is referred to a epipolar alignment or orienting stereo pair. The epipolar alignment can be achieved by bringing down or transforming the points on the images to the corresponding ground control points.

In this study, the epipolar geometry of stereo is established using non-parametric method, i.e., using a number of GCPs and three algorithms and applying least-square principles. This approach uses mathematical relationships between the positions of pixels in an image and the corresponding positions of those points on the real-world coordinates. The advantage of this approach is that it corrects the image geometry

1986). Three algorithms developed from the approach include: (1) Affine Transformation, (2) Projective Transformation, (3) Polynomial Transformation (Moffit and Mikhail, 1980).

Affine Transformation

In this transformation two scale factors S_x and S_y , non perpendicular (affinity) δ between two axis to be rotated by angle θ , and two translation parameters (change of position) between two systems, are affected. Figure 2.1 shows rotation and translation of two-dimensional coordinate system.

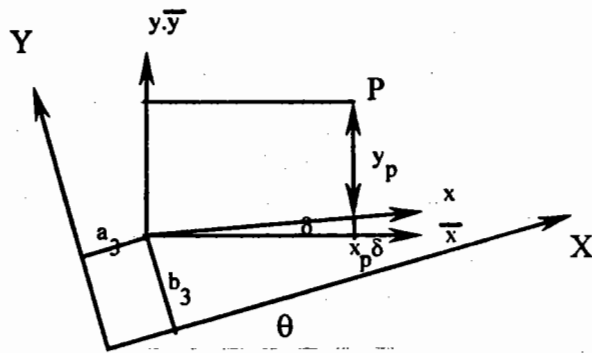


Figure 2.1. Transformation of non orthogonal image (x,y) to orthogonal map (X,Y).

From Figure 1 above δ is very small, so that the approximation of $\sin \delta = \delta$ and $\cos \delta = 1$

Hence:

$$\begin{aligned} \bar{x}_p &= x_p \cos \delta = x_p \\ \bar{y}_p &= y_p + x_p \sin \delta \\ &= y_p + x\delta \end{aligned}$$

$$\begin{bmatrix} \bar{x} \\ \bar{y} \end{bmatrix} = \begin{bmatrix} 1 & 0 \\ \delta & 1 \end{bmatrix} \begin{bmatrix} x \\ y \end{bmatrix} \text{ is the orthogonal image coordinate system.}$$

Applying scale changes S_x and S_y to x and y respectively, we have the scaled orthogonal image:

$$\begin{bmatrix} \bar{x} \\ \bar{y} \end{bmatrix} = \begin{bmatrix} 1 & 0 \\ \delta & 1 \end{bmatrix} \begin{bmatrix} S_x & x \\ S_y & y \end{bmatrix}$$

The scaled orthogonal image is then rotated by θ and translated by a_3 and b_3 . This has resulted in the ground coordinate system as follow.

$$\begin{bmatrix} X \\ Y \end{bmatrix} = \begin{bmatrix} \cos \theta & -\sin \theta \\ \sin \theta & \cos \theta \end{bmatrix} \begin{bmatrix} \bar{x} \\ \bar{y} \end{bmatrix} + \begin{bmatrix} a_3 \\ b_3 \end{bmatrix}$$

$$\begin{bmatrix} X \\ Y \end{bmatrix} = \begin{bmatrix} a_1 & a_2 \\ b_1 & b_2 \end{bmatrix} \begin{bmatrix} x \\ y \end{bmatrix} + \begin{bmatrix} a_3 \\ b_3 \end{bmatrix},$$

where:

$$\begin{aligned} a_1 &= S_x (\cos \theta - \delta \sin \theta) \\ a_2 &= -S_y \sin \theta \\ b_1 &= S_x (\sin \theta + \delta \cos \theta) \\ b_2 &= S_y \cos \theta \end{aligned}$$

The above equation is known as Affine transformation that is used to transform a non-orthogonal image system (x,y) to an orthogonal ground system (X,Y).

In the implementation of the Affine transformation, we assume that the satellite image coordinate system identified on the computer screen monitor is non-orthogonal, and the ground coordinate system derived from a topographic map is orthogonal.

Projective Transformation

The Projective Transformation is also known as eight-parameter transformation. In this report, the formula derivation of this algorithm is not provided. The implementation of the algorithm is as follow (Figure 2.2).

The projectivity equations:

$$X = \frac{a_1x + a_2y + a_3}{c_1x + c_2y + 1}$$

$$Y = \frac{a_4x + a_5y + a_6}{c_1x + c_2y + 1}$$

X, Y : Ground Coordinate System
x, y : Image Coordinate System

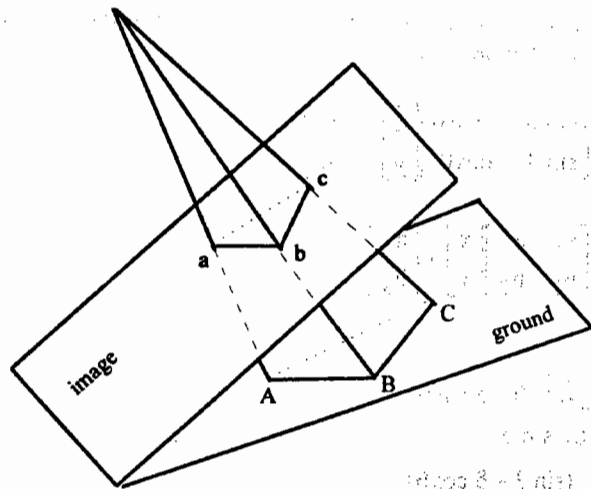


Figure 2.2. Projectivity between plane I (image) and plane II (ground).

In the implementation of projectivity equation, we assume that a perspective relationship between image and ground system exists.

Polynomial Transformation.

This method is used to transform and correct the distortion of image relative to a dense set of control points. The order of the polynomial depends on the number of the control points available. The more control points available, the more accurate the result of the transformation (rectification) will be. As mention-before, this approach is a non-parametric, so it is completely independent of the geometry of the satellite.

Using the polynomial transformation, the original image will be shifted, rotated, scaled, and squeezed so that it fits best following the least square principle to the given reference points (GCPs).

This polynomial transformation is used most often for satellite images, whose geometry and distortion are some time difficult to model. The relief displacement can be neglected since the topography of the earth is relatively small compared to the satellite flying height. Therefore, in this study we consider only x,y coordinates. The equations of polynomial transformation are:

$$X = x^t Ay$$

$$Y = y^t By$$

$$x^t = \begin{bmatrix} 1 & x & x^2 & x^3 & \dots \end{bmatrix}$$

$$y^t = \begin{bmatrix} 1 & y & y^2 & y^3 & \dots \end{bmatrix}$$

$$A = \begin{bmatrix} a_{00} & a_{01} & a_{02} & \dots \\ a_{10} & a_{11} & a_{12} & \dots \\ a_{20} & a_{21} & a_{22} & \dots \\ \vdots & \vdots & \vdots & \dots \end{bmatrix} \quad B = \begin{bmatrix} b_{00} & b_{01} & b_{02} & \dots \\ b_{10} & b_{11} & b_{12} & \dots \\ b_{20} & b_{21} & b_{22} & \dots \\ \vdots & \vdots & \vdots & \dots \end{bmatrix}$$

For example, if 3rd degree polynomial used, then :

$$X = a_{00} + a_{10}x + a_{20}x^2 + a_{01}y + a_{11}xy + a_{21}x^2y + a_{02}y^2 + a_{12}xy^2 + a_{22}x^2y^2$$

$$Y = b_{00} + b_{10}x + b_{20}x^2 + b_{01}y + b_{11}xy + b_{21}x^2y + b_{02}y^2 + b_{12}xy^2 + b_{22}x^2y^2$$

2.2 Computation of B/H ratio

In the effort to compute the B/H ratio, the space-resection method based on collinearity condition between image points and their corresponding GCPs (Wolf, 1974) has been chosen (Figure 2.3). This step is intended to determine the exterior orientation of the satellite at the time of observation.

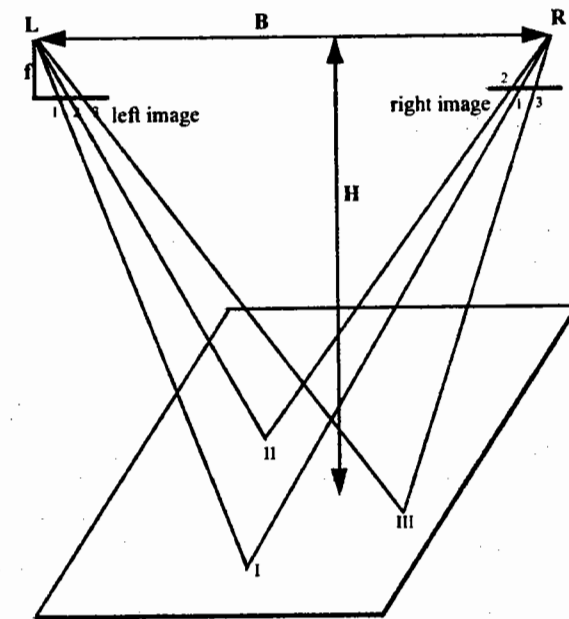


Figure 2.3. Geometry of Space Resection

Based on the geometry shown in Figure 3.3, we have:

X_L, Y_L, Z_L and X_R, Y_R, Z_R are satellites coordinates at the time of exposure of left and right images respectively.

$$x_i = -f \frac{r_{11}(X_i - X_0) + r_{12}(Y_i - Y_0) + r_{13}(Z_i - Z_0)}{r_{31}(X_i - X_0) + r_{32}(Y_i - Y_0) + r_{33}(Z_i - Z_0)}$$

$$y_i = -f \frac{r_{21}(X_i - X_0) + r_{22}(Y_i - Y_0) + r_{23}(Z_i - Z_0)}{r_{31}(X_i - X_0) + r_{32}(Y_i - Y_0) + r_{33}(Z_i - Z_0)}$$

where:

- x_i, y_i = image coordinates of point I
 X_i, Y_i, Z_i = GCPs coordinates
 X_0, Y_0, Z_0 = position of the sensor, i.e., X_L, Y_L, Z_L and X_R, Y_R, Z_R for left and right images respectively
 $r_{11}, r_{12}, \dots, r_{33}$ = nine elements of rotation as function of ω, ϕ, κ (orientation of the sensor)
 f = focal length of the sensor

Accordingly, the values of B and H are:

$$B = [(X_R - X_L)^2 + (Y_R - Y_L)^2 + (Z_R - Z_L)^2]^{1/2}$$

$$H = (Z_R + Z_L)/2$$

3. MATERIAL AND METHODS

3.1 Material

This study used a pair of overlapped AVNIR images. The technical specifications of these images are as follow:

Image 1 (Left Image):

- Satellite: ADEOS
- Sensor: AVNIR Pan
- Observation date: 1997/05/10
- GRS Column-Line: 1355- 355
- RSP Path-Frame: 65- 290
- Scene Shift Rate: 3
- Angle of Pointing: -2.20
- Cloud Coverage: 00
- Ground Station: HEOC
- Product Code: L1BP
- Processing Level: 1B1
- Earth Ellipsoid: Tokyo
- Center Latitude: N 35.121
- Center Longitude: E135.570
- Number of Pixels: 10000
- Number of Lines: 10000
- Data Size (MB) : 98.4
- Logical Format: CEOS-BSQ
- Physical Format: ISO9660
- Record Format: ISO9660
- Media: CD-ROM
- Number of Vol.: 1
- W/O No.:D9750061-002
- Master Media No.: D129000075
- Production date: 1997/12/03

Image 2 (Right Image):

- Satellite: ADEOS
- Sensor: AVNIR Pan
- Observation date: 1996/12/30
- GRS Column-Line: 1355- 350
- RSP Path-Frame: 71- 289
- Scene Shift Rate: 0
- Angle of Pointing: 18.81
- Cloud Coverage: 01
- Ground Station: HEOC
- Product Code: L1BP
- Processing Level: 1B1
- Earth Ellipsoid: Tokyo
- Center Latitude: N 35.220
- Center Longitude: E135.423
- Number of Pixels: 10000
- Number of Lines: 10000
- Data Size (MB) : 98.4
- Logical Format: CEOS-BSQ
- Physical Format: ISO9660
- Record Format: ISO9660
- Media: CD-ROM
- Number of Vol.: 1
- W/O No.:D9750061-001
- Master Media No.: D129000075
- Production date: 1997/12/01

In addition, topographic maps (scale 1 : 50,000) of the area covered by the images were used to obtain ground control points.

3.2 Methods

Digital Rectification

In order to apply the transformation algorithms, two major steps: (1) Identification of the Ground Control Points (GCPs) and (2) Identifications of corresponding points on the images. Ground control points were selected based on the following criteria:

- They must be easily identified on both images as well as on the topographic maps
- They must be evenly distributed in the study area.

This study selected 26 GCPs that match the criteria. The GCPs identified on the topographic maps were digitized and their coordinates were transformed into UTM coordinates using facilities available in the ARC/INFO GIS package program. On the other hand, the identification of the GCPs on the images was done using the ER Mapper Image Processing System. Once the GCPs were identified on both maps and images, they were used as input in the coordinate transformation processes as described in the methodology.

B/H Ratio Computation

The values GCPs on the ground coordinates and the values of corresponding points on the image coordinate were also used as input into the collinearity conditions equation to determine the positions of the sensors that generated left and right images. In this case, linearization of the equations was done using Taylor's theorem with 10 iterations.

4. RESULTS AND DISCUSSION

Twenty five GCPs coordinates were identified on the topographic maps and on the

accuracy and provided a comparable RMSE. Those are summarized in Table 4.1. The results are not very surprising in the case that the RMSEs are larger than 50 m even though the resolution of AVNIR data is designed to reach 8 m. The most probable causes of the large RMSE can be attributed to (1) the use of topographic map at a 1 : 50000 scale as the source of GCPs values, (2) the poor quality of the images, and (3) the authors' unfamiliarity with the area covered on the images (Kyoto Area).

It is not an easy task to achieve the accuracy of less than 50 m in identifying GCPs using map with the scale of 1 : 50000 (the results have indicated that the accuracy is equivalent with 1-2 mm on a map at a 1 : 50,000 scale). The quality of the images, particularly the tone, is not good. This has made it difficult to identify corresponding points of the GCPs on the images. Moreover, the image observation dates are about 6 months different (the right image was taken in December 1996 and the left was in May 1997). In this case, some parts of the right image are blank and looks white -- possibly snow covered.

Table 4.1. RMSE of the two sets of identified GCPs on Image 1 (Left) and Image 2 (Right)

	Image 1 (Left)	Image 2 (Right)
Affine	53.889 m	112.249 m
Projective	53.023 m	77.026 m
Polynomial	66.375 m	91.253 m

In order to determine the B/H ratio of the two images, the satellite sensor positions were first computed using collinearity conditions. Since the authors did not have the information about the values of AVNIR focal length (f), this assessment used the value of f = 1082 mm

The linearization of the equation done using Taylor's theorem shows the convergence of the the exterior orientation parameters values of both images. Figure 4.1a and 4.1b respectively show the convergence of delta omega ($\Delta\omega$), delta phi ($\Delta\phi$), delta kappa ($\Delta\kappa$), and delta X (ΔX), delta Y (ΔY), and delta Z (ΔZ) of the left image. Figure 4.2a and 4.2b respectively show the convergence of delta omega ($\Delta\omega$), delta phi ($\Delta\phi$), delta kappa ($\Delta\kappa$), and delta X (ΔX), delta Y (ΔY), and delta Z (ΔZ) of of the right image.

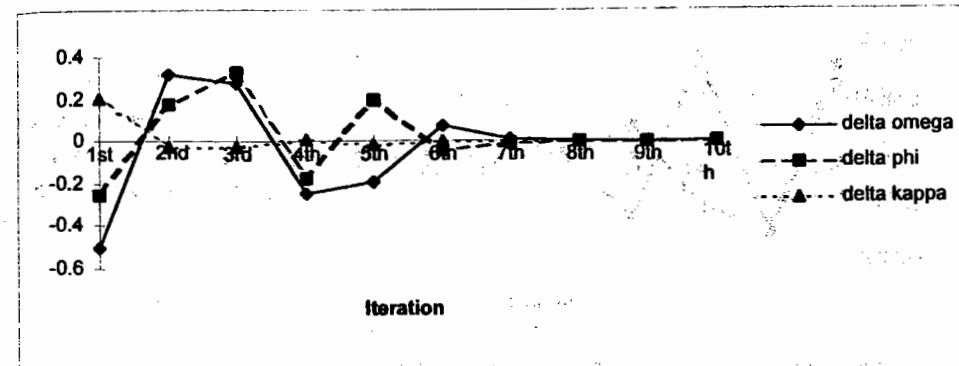


Figure 4.1a. The convergence of delta omega ($\Delta\omega$), delta phi ($\Delta\phi$), delta kappa ($\Delta\kappa$) of the left image as a result of 10 iterations.

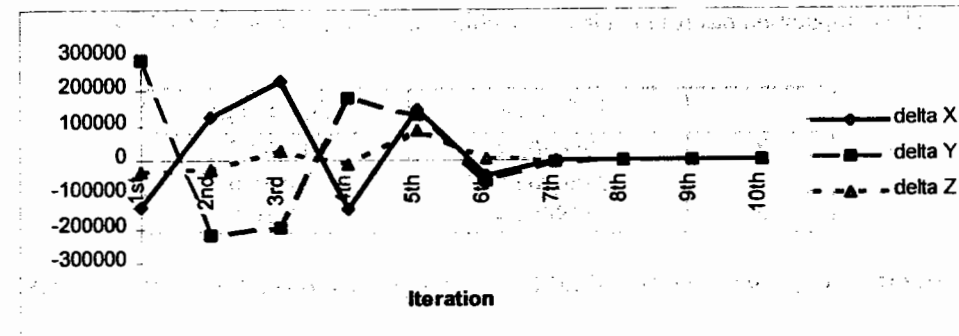


Figure 4.1b. The convergence of delta X (ΔX), delta (ΔY), and delta (ΔZ) of the left image as a result of 10 iterations.

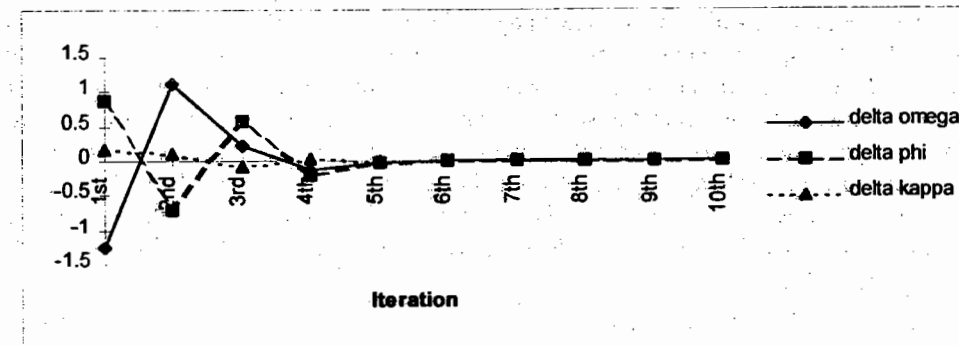


Figure 4.2a. The convergence of delta omega ($\Delta\omega$), delta phi ($\Delta\phi$), delta kappa ($\Delta\kappa$) of the right image as a result of 10 iterations.

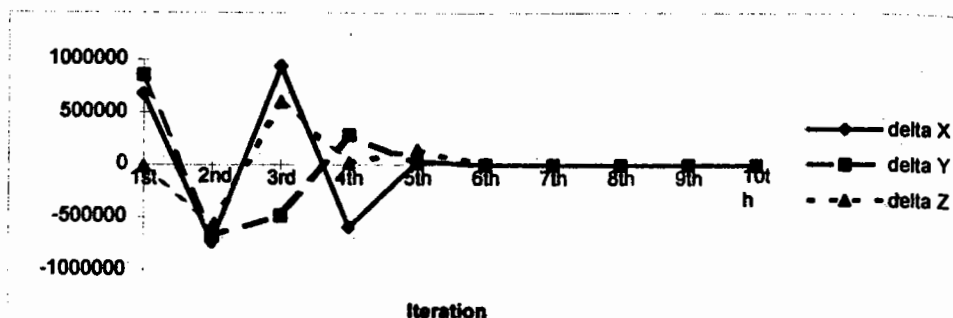


Figure 4.2b. The convergence of delta X (ΔX), delta (ΔY), and delta (ΔZ) of the right image as a result of 10 iterations.

The computation has resulted in the Satellite Coordinates (meters) as follow:

	Left Image	Right Image
X	366305.4	202559.7
Y	3766906.0	3894686.0
Z	619052.4	580710.5

so that $B = 211211.9$ m, and $H = 599881.4$ m. Therefore the B/H ratio is $B/H = 0.352089$.

5. CONCLUSION

The results summarized in this research show that the planimetric accuracy (RMSE) emerged as a result of the digital rectification using three algorithms are difficult to evaluate the real capability of AVNIR images. The values of RMSE that exceed 50 m do not reflect the spatial accuracy of AVNIR as announced by NASDA. This is mainly because the GCPs used in this research were obtained from topographic maps which their planimetric accuracy is below the spatial resolution of the AVNIR images. Nevertheless, since this preliminary study used only a pair of overlapped images, the study is needed to be extended if the real capability of AVNIR images needs to be established. This can be done, for example by using other overlapped images of different areas that cover various terrain, and also using sets of GCPs with better accuracy and with differing GCPs distribution in the area.

Regarding the B/H ratio computation, the authors conclude that the performance of AVNIR data is good as reflected on the convergence of the results. However, the authors also realize that the underlying assumption that the images have central projection is not entirely true. The pushbroom type sensor of AVNIR demands more rigorous algorithm that includes time dependent exterior orientations in each image.

6. ACKNOWLEDGMENTS

The authors would like to thank the UN ESCAP-NASDA research program that has provided funding for this research. The authors would also like to acknowledge the support from the Department of Geodetic Engineering Faculty of Engineering, Gadjah Mada University, Yogyakarta, Indonesia to conduct this research. Special thanks goes to Professor Shunji Murai of University of Tokyo and Asian Institute of Technology Bangkok who encourages the authors to do and continue this research.

7. REFERENCES

- Kurt Novak (1992). *Rectification of Digital Imagery*. PE & RS, Vol. 58, No.3, March 1992, pp. 339-344.
- Liang Chien Chen and Liang Hwei Lee (1993). *Rigorous Generation of Digital Orthophotos from SPOT Images*. PE & RS, Vol.59, No.5, May 1993, pp. 655-661.
- Moffit, Francis H. and Mikhail, Edward M. (1980) *Photogrammetry (Third Edition)*. New York (Harper & Row), Publisher.
- Nakamura, Yasuhisa (1997). ADEOS Program. *Geocarto International*, Vol. 12, No. 4. pp. 7-14.
- Rao, T.Ch. Malleswara, Rao K. Venugopala, Kumar, A. Ravi; Rao, D.P.; and Deekshatula, B.L. (1996) *DTM from IRS Data*. PE & RS, Vol.62, No.6, 1996, pp. 727-731.
- Toshiaki, Hashimoto (1997). DEM Generation from AVNIR Stereo Images. *Geocarto International*, Vol. 12, No. 4. pp. 35-37.
- Wolf, Paul R. (1974). *Elements of Photogrammetry*, International Students Edition, McGraw Hill, Kogakusha Ltd., Tokyo.

